Active damping of the 1D rocking mode

Bayan Babakhani and Theo J. A. de Vries

***Abstract*— Active damping of a rotational vibration mode in the linear guidance of a precision machine in a one dimensional (1D) setting is considered in this paper. This so-called rocking mode presents itself in machines having linear actuation. The limitation this vibration mode imposes on the machine precision and closed-loop bandwidth can be overcome by means of active damping. Implementing active damping in a collocated fashion in combination with a passive control algorithm guarantees the robust stability of the system. Active damping control operates in parallel with the motion controller if one is present. These controllers operate completely independently of each other. The overall result is that a higher bandwidth can be achieved for the closed-motion-loop involving the actively damped plant. This improves the performance of the machine in terms of response time, settling time and steady-state and/or set-point error.**

I. Introduction

Precision machines are designed to be light, fast and accurate. Damping in these machines is either left out intentionally e.g. to avoid design inaccuracies or just overlooked. This results in high-frequency resonances that limit the achievable bandwidth and hence limit the performance of such machines in terms of both speed and accuracy.

An example of such a situation is a machine fitted with linear actuators. The guidance system on such actuators has a certain compliance. This compliance in the guidance causes rotational vibrations: the so-called 'Rocking mode'. Such rotational vibrations cause uncertainty in the position of the end-effector that is mounted on the linear guidance, as the end-effector shows a badly damped oscillation in its response. The long settling time of the end-effector in some plants, such as pick-and-place machines and cutting machines, causes significant time loss. Given that high-precision machines cannot allow such inaccuracies, the operation is paused until the vibrations are damped.
Another problem may occur when a motion controller is added to these machines in order to improve the system performance. Preferably, the motion controller should have a low-pass characteristic in order to suppress high-frequency disturbances. However, adding such a feedback motion controller to this type of plant is only possible in combination with a low gain and low bandwidth. For high loop gains, the complex poles present in the loop transfer migrate to the open right half of the complex plane. Since the poles have low damping, which means they are very close to the imaginary axis, even a small loop gain can destabilize the system.

A possible solution to this problem is to add active damping to the system at the resonance frequencies. Active damping flattens the resonance-peak in the transfer function of the system. By damping resonance peaks, the bandwidth of the system can increase without the danger of instability. In turn, this allows for higher integral gain in the motion control algorithm.

This paper describes the rocking mode and the effects of active damping in the one-dimensional setting. It starts by describing a general plant model in section II followed by a one dimensional (1D) model of the rocking mode phenomenon in section III. Collocated and non-collocated control are discussed in section IV leading to the design procedure for both motion controller (section V-A) and active damping (section VI). This paper concludes by presenting the results and the conclusions drawn from them.

II. Plant model

A dynamic model of the plant is assumed to be given in terms of a modal decomposition, which is an intuitive way of representing the dynamics of a system. In such a representation, a general plant transfer function can be obtained by summation of all the modal contributions. The reader is referred to [1] for more extensive information and theoretical background of modal analysis.
Consider $\mathbf{F}_x$ to be the vector of the generalized forces on a plant, and $\mathbf{x}$ to be the generalized coordinates. The transfer function from the local force $F_{x,j}$ (the j-th element of $\mathbf{F}_x$) to the local position x_k (the k-th element of $\mathbf{x}$) is the sum of each modal contribution, which in turn is determined by the mode-shape vector elements, ϕ_{ij} and ϕ_{ik}:

$$\frac{x_k}{F_{x,j}}(j\omega) = \sum_{i=1}^{n} \frac{\phi_{ij}\phi_{ik}}{m_{m,i}(j\omega)^2 + d_{m,i}(j\omega) + k_{m,i}} \qquad (1)$$

Here, $m_{m,i}$, $d_{m,i}$ and $k_{m,i}$ respectively represent modal mass, damping and stiffness of the i-th mode. $d_{m,i}$ is determined by the modal damping ratio, ξ_i, according to:

$$d_{m,i} = 2\xi_i m_{m,i}\omega_{e,i} \qquad (2)$$

The authors gratefully acknowledge the support of the Smart Mix Programme of the Netherlands Ministry of Economic Affairs and the Netherlands Ministry of Education, Culture and Science.

Bayan Babakhani is with Faculty of Electrical Engineering, Mathematics and Computer Science, University of Twente, 7500 AE Enschede, The Netherlands. b.babakhani@utwente.nl

Theo J. A. de Vries is with Faculty of Electrical Engineering, Mathematics and Computer Science, University of Twente, 7500 AE Enschede, The Netherlands. t.j.a.devries@utwente.nl

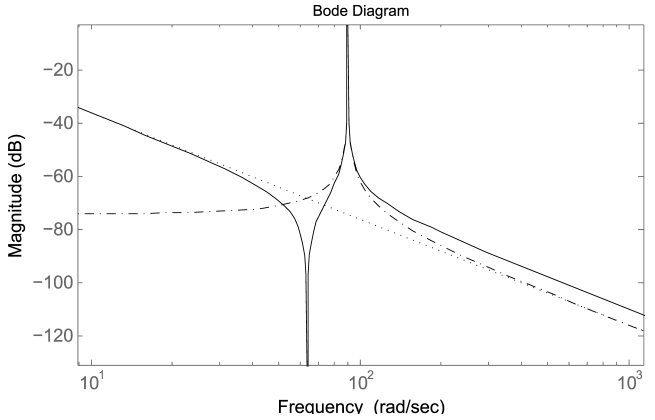

Fig. 1. Magnitude plot: rigid-body mode (dotted), 1^{st} flexible mode at $\omega_e = 90 rad/s$ (dashed) and the resulting 4^{th}-order plant transfer function (solide line)

Furthermore, the resonance frequency of the i-th mode, $\omega_{e,i}$, is equal to:

$$\omega_{e,i} = \sqrt{\frac{k_{m,i}}{m_{m,i}}} \tag{3}$$

A. Model Reduction

To simplify the plant model, model reduction is usually applied to high-order plant models. This results in a model having the rigid body mode and the flexible modes that have a significant influence on the dynamic behavior of the plant in the frequency region of interest. Here, we consider a fourth order plant having a rigid body mode ($i = 0$) and a flexible mode ($i = 1$), as shown in figure 1. Here, $m = 0.633$kg, $\omega_e = 90$rad/s, $\omega_a = \omega_e/\sqrt{2}$ and $\xi = 0.1\%$. The transfer functions of this plant can be obtained using (1):

$$\begin{aligned}\frac{x_k}{F_{x,j}}(j\omega) &= \frac{1}{m_{m,0}(j\omega)^2} + \frac{\phi_{1j}\phi_{1k}}{m_{m,1}(j\omega)^2 + d_{m,1}(j\omega) + k_{m,1}} \\ &= \frac{(1+\alpha)(j\omega)^2 + 2\xi\omega_e(j\omega) + \omega_e^2}{m(j\omega)^2\left((j\omega)^2 + 2\xi\omega_e(j\omega) + \omega_e^2\right)}\end{aligned} \tag{4}$$

where:

$$\begin{aligned}\alpha &= \frac{m_{m,0}}{m_{m,1}}\phi_{1j}\phi_{1k} \\ m &= m_{m,0}\end{aligned} \tag{5}$$

B. Frequency ratio α

In general, α_i is the factor relating $\omega_{e,i}$ and $\omega_{a,i}$ of the i-th mode of a plant according to:

$$\omega_{a,i}^2 = \frac{\omega_{e,i}^2}{1+\alpha_i} \tag{6}$$

In a mechanical system, α is determined by the location of the sensor w.r.t. the actuator. As α decreases, the zeros in the pole-zero plot move up along the imaginary axis toward infinity where they disappear, to appear again on the real axis when α decreases further [2] [3]. The position of the zeros w.r.t. the poles determines the type of the plant transfer function. Table I shows all the possible ranges of α and the corresponding types of plant transfer functions as discussed in [4].

TABLE I

PLANT TYPES

α	Plant transfer function type	Characteristic
$\alpha > 0$	Anti-resonance - Resonance (AR)	$\omega_a < \omega_e$
$\alpha = 0$	Double integrator(D)	$\omega_a = \omega_e$
$-1 < \alpha < 0$	Resonance - Anti-resonance (RA)	$\omega_a > \omega_e$
$\alpha = -1$	Resonance (R)	$\omega_a = \inf$
$\alpha < -1$	Non-minimum phase (N)	zeros at $\pm\omega_a$

III. ROCKING MODE

We are investigating the rotational vibrations modes in systems with flexible guiding. Figure 2 shows a schematic, one-dimensional (1D) representation of this situation. It shows a plant, having a mass m and inertia J, mounted on a flexible guidance of a linear actuator. This guidance has a stiffness c, and very low damping (typical value of 0.1% according to [5]). The actuator force, F, is applied to the system in order to initiate a translational movement, x. In addition to this translation, F also excites a rocking mode around the center of mass, COM. This causes a ripple on the measured position of the end-effector, which limits the performance of the machine.

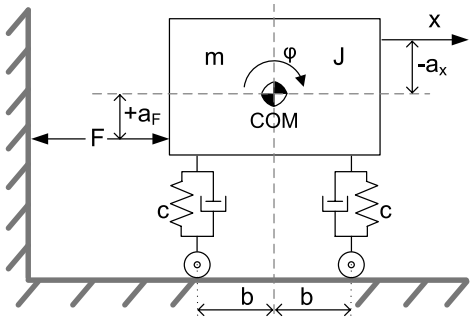

Fig. 2. 1D model of a plant with rocking mode

The transfer function of such a plant is given by equation (8):

$$\begin{aligned}\frac{x}{F}(j\omega) &= \frac{1}{m(j\omega)^2} + \frac{a_F a_x}{J(j\omega)^2 + 2\xi\omega_e(j\omega) + k} \\ &= \frac{(1+\alpha)(j\omega)^2 + 2\xi\omega_e(j\omega) + \omega_e^2}{m(j\omega)^2\left((j\omega)^2 + 2\xi\omega_e(j\omega) + \omega_e^2\right)} \\ &= \frac{1}{m(j\omega)^2}\cdot\frac{(j\omega)^2 + 2\xi_a\omega_a(j\omega) + \omega_a^2}{(j\omega)^2 + 2\xi\omega_e(j\omega) + \omega_e^2}\cdot\frac{1}{(1+\alpha)} \\ &= \frac{1}{m(j\omega)^2}\cdot\frac{(j\omega)^2 + 2\xi_a\omega_a(j\omega) + \omega_a^2}{(j\omega)^2 + 2\xi\omega_e(j\omega) + \omega_e^2}\cdot\frac{\omega_r^2}{\omega_a^2}\end{aligned} \tag{7}$$

$$P(s) = \frac{1}{ms^2}\cdot\frac{s^2 + 2\xi_a\omega_a s + \omega_a^2}{s^2 + 2\xi\omega_e s + \omega_e^2}\cdot\frac{\omega_e^2}{\omega_a^2} \tag{8}$$

TABLE II

CONDITIONS ON THE PLANT TYPE

Type	α	Condition
AR	$\alpha > 0$	$a_F a_x > 0$
D	$\alpha = 0$	$a_F a_x = 0$
RA	$-1 < \alpha < 0$	$a_F a_x < 0$
R	$\alpha = -1$	$J + m a_F a_x = 0$
N	$\alpha < -1$	$J + m a_F a_x < 0$

where:

$$\begin{aligned} k &= 2cb^2 \\ \alpha &= \frac{m}{J} a_F a_x \\ \xi_a &= \frac{\xi}{\sqrt{1+\alpha}} \\ \omega_a &= \sqrt{\frac{k}{J + m a_F a_x}} \\ \omega_e &= \sqrt{\frac{k}{J}} \end{aligned} \tag{9}$$

As can be seen, the anti-resonance frequency depends on the positions of actuator and sensor; more specifically, on their distance to the COM, a_F and a_x. Table II shows the type of the transfer function for different values of a_F and a_x.

IV. CONTROL

A. Collocated control

Collocated control means that the sensor and actuator in the control loop are energetically conjugated. In the mechanical sense, this means that the sensor and actuator are physically at the same place or that there is only a rigid link between the sensor and actuator [2]. A collocated sensor and actuator pair forms a power port between the controller and the plant. This makes it possible to control the power flow to the plant.

In pole-zero terms, collocated control in a lightly damped flexible structure leads to alternating poles and zeroes near the imaginary axis. One advantage of this alternation is that the zeros compensate the undesirable phase lag caused by the poles [2]. Another advantage is that the root-locus plot keeps the same general shape and stays within the left-half plane, despite possible variations that might be large [3].

Collocated actuator and sensor, in combination with either an intrinsically passive or a dissipative control, guarantees the stability of the control system. This of course only applies if there are no limitations imposed by the electronics, actuators and sensors used.

B. Non-collocated control

When non-collocated control is applied, sensing and actuation take place at different parts of the plant. Unlike for collocated control, there is no stability guarantee for non-collocated control. This makes non-collocated control less robust against parameter variations and discrepancies between the plant model used and the actual plant. On the other hand, when the state to be controlled is measured directly, a better performance can be achieved than when the state of interest is deduced from a measurement performed where the actuator is located (collocated measurement).

V. MOTION CONTROL

It is decided to implement a PID motion controller, which is a widely implemented motion controller in industrial applications. The motion control design is described in the following subsections, by presenting the tuning method used (V-A) and describing the placement of the actuator and sensor (V-B).

A. Motion Control Algorithm

The motion controller is tuned on the basis of the moving mass transfer function, which is:

$$P_{mass}(s) = \frac{1}{ms^2} \tag{10}$$

To reduce high-frequency gain, a low-pass filter is added to the controller that adds extra high-frequency roll-off. This combination is termed PID+, where the '+' sign refers to the additional low-pass filter. PID+ has the following general transfer function:

$$C_{PID+}(s) = k_P \frac{(s\tau_D + 1)(s\tau_I + 1)}{\left((s\beta\tau_D)^2 + 2\zeta s\beta\tau_D + 1\right) s\tau_I} \tag{11}$$

where $\beta = 0.1 \cdots 0.7$ is the tameness constant of the differentiation action within the motion controller and $\zeta = 0.7 \cdots 0.9$ represents the relative damping of the motion controller.

The open-loop cross-over frequency, ω_c, which is directly related to the desired closed-loop bandwidth, is chosen according to the target performance. The performance requirements can put a restriction on either the set-point or tracking error or aim for a certain level of disturbance rejection. This, in combination with the desired dynamic behavior that is determined by the reference signal, results in a minimum required ω_c. Using this ω_c and the rigid-body mass of the plant, m, the parameters of the motion controller can be determined according to the following tuning rules [6]:

$$\begin{aligned} k_P &= m\omega_c^2\sqrt{\beta} \\ \tau_D &= \left(\omega_c\sqrt{\beta}\right)^{-1} \\ \tau_I &\geq 2\tau_D \end{aligned} \tag{12}$$

Hence, the central parameter, by which performance and stability are tuned, is ω_c.

Figure 3 shows the bode plot of such a controller. Here $\beta = 0.1$, $\zeta = 0.7$, $m = 0.633\,kg$ and $\omega_c = 50\,rad/s$.

As a result of the low-pass filter implemented, this motion controller is not passive. Therefore, its combination with collocated sensor and actuator does not guarantee stability. Non-collocated motion control, where the position of the end-effector is measured directly, is in fact more appealing in this case, since it leads to a better performance than collocated motion control (see section IV-B).

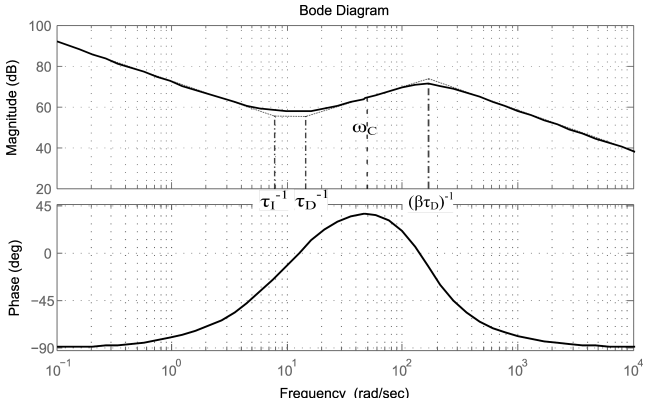

Fig. 3. Bode plot of PID+ controller

Figure 4 shows the root-locus of the system containing the above mentioned plant and controller, for ω_c varying between 1 and ∞ [8]. So the system parameter used as the variable is not the loop gain, but the less commonly used ω_c. The root-locus shows that the closed-loop system is only stable for low ω_cs. The closed-loop poles appear to enter the left hand side of the complex again, once ω_c is increased beyond a certain boundary. However, in reality, there are high order modes present that prevent the system from stabilizing. Such modes were not modeled here and therefore do not influence the root-locus as shown in 4.

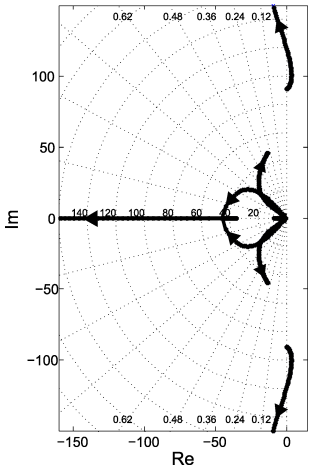

Fig. 4. Pole-zero plot of the plant in combination with a PID+ motion controller, no active damping

B. Sensor and Actuator Location

The position of the actuator w.r.t. the COM is generally determined by the machine structure. The moving part of the plant is usually mounted on top of the linear actuator. This means that both the sign and the magnitude of a_F are already determined (below the COM).

As Table II shows, a_F and a_x together determine the type of the plant transfer function and thus its stability properties. It is usually easier to determine or change the position of the sensor rather than the position of the actuator. Depending on the desired transfer function type, the sensor should be positioned w.r.t. the COM. However, the exact location of the COM is usually unknown and it might be prone to change due to parameter variations, e.g. a change in the machine state. Therefore, a_x should be chosen to be large enough to make the transfer function robust against these uncertainties and thus prevent type switching.

[7] shows that the AR type plant in combination with sufficient modal damping is stable for a wider range of ω_c than the RA type. It also shows that an α close to 0 is beneficial for closed-loop stability. An α close to 0 requires a low product of a_F and a_x.

It is important to realize that if enough damping can be added to the system at the resonance and anti-resonance frequencies such that the system shows the characteristics of a moving mass, the considerations above will no longer be critical. Since the plant increasingly resembles a moving mass when localized damping is increased, the performance of the implemented PID+ motion controller, which is designed for a moving mass, improves.

VI. Active damping

A. Location of Active Damping Unit

Figure 2 shows that our plant consists of three main parts; the actuator (linear motor), the guidance system and a moving part. Ideally, the damping should be applied between the moving part and the guidance system of the actuator. This is where the compliance causing the rocking mode is located. However, it should be clear that this is physically impossible. In practice, there should be a platform on which an active damping device can be mounted. For this, we divide the moving part of the machine into two parts: a lightweight carriage and the rest of the linearly actuated part (containing the end-effector) called the head. The active damping unit (ADU) can be placed in between these two parts, as shown in Figure 5.

The carriage's mass should be chosen to be low enough to result in a very high resonance frequency compared to the resonance frequency of the head. If this high order dynamic is neglected, there is no need to take the inertia of the carriage into account. After dividing the plant, it consists of a linear actuation, the carriage (translational mass, m_c), the ADU and the head (both mass m_h and inertia J).

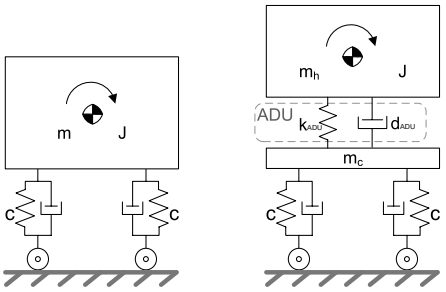

Fig. 5. Schematic view of the ADU location in the plant

B. The Active Damping Algorithm

The desired movement for the plant is a strictly translational one. This means that in absence of the rocking mode, there should be no torque between the carriage and the head. Assuming that the rotational vibration of the carriage is negligible (see section VI-A, it could be considered as the fixed world in the rotational sense. Active damping can be applied by measuring the torque between the two moving parts, namely the carriage and the head, and counteracting it using a position actuator that is mounted on top of the previously mentioned sensor. For both actuator and sensor, we envision the use of piezo. The previously described ADU implements a collocated control concept, as there is no energy storage between the sensor and the actuator. By applying an intrinsically passive controller (IPC), the stability of the plant -including active damping- is guaranteed (see section IV-A):

For active damping, a Leaking Integral Force Feedback,

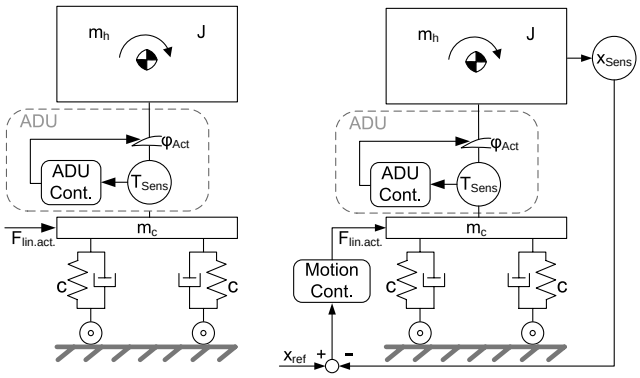

Fig. 6. Schematic view of the plant in combination with both ADU and motion controller

LIFF, (13) has been applied to the plant.

$$\begin{aligned} C(s) &= \frac{K_{LIFF}}{s + p_{LIFF}} \\ d_{ADU} &= \frac{1}{K_{LIFF}} \\ k_{ADU} &= \frac{p_{LIFF}}{K_{LIFF}} \end{aligned} \tag{13}$$

This controller behaves as a mechanical damper, d_{ADU}, for high-frequencies (higher than p_{LIFF}) and as a stiffness, k_{ADU}, for low frequencies. Thus we have a damper and stiffness in parallel, placed in between the head and the carriage. This controller, called the ADU controller, operates in parallel with but independently of the motion controller, if one is present. The parameters of the ADU controller have been tuned according to the rules of thumb deduced in [5]. This tunning method merely uses the resonance and anti-resonance frequencies of the head, and hence excludes any model uncertainty. The maximum amount of damping depends on the resonance frequency, its ratio to the anti-resonance frequency and the actuator-sensor stack compliance.

As can be seen from Figure 7, the implemented ADU adds damping to the complex poles and zeroes of the plant. It also adds extra dynamics, belonging to its actuator and sensor, to the system.

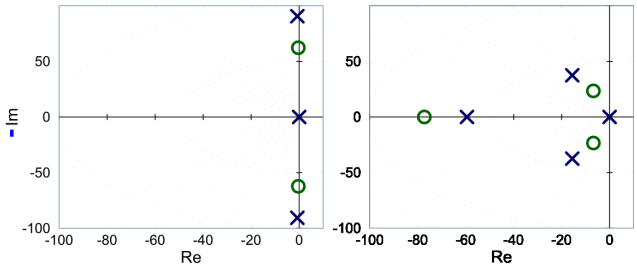

Fig. 7. Pole-zero plot, with and without active damping

VII. Results

To show the effect of active damping on the system performance, a number of simulation were performed, the results of which are discussed in this section.

The plant model is the same as already explained inII, with $\omega_e = 90.62$ rad/s and $\omega_a = 62.29$ rad/s. In all the simulations discussed here, acceleration feed-forward was applied to the plant. The acceleration profile is scaled with a factor representing the plant's rigid body mass, to obtain the input force that is applied to the plant by the linear actuator. To mimic the model uncertainty that is present in reality, this scaling factor has been chosen to be 5% lower than the rigid body mass of the plant model. Other model discrepancies with the actual plant, such as friction, are not taken into account during the simulations. The acceleration profile is chosen such that it should lead to a displacement of $0.5m$.

A. Plant response

First, the effect of active damping on the plant response is investigated. As expected, the results shown in figure 8 show a set-point error equal to $0.025\ m$.

This figure also shows the reduce of the oscillatory behavior due to the added active damping. After $8.95\ s$, the vibration amplitude of the plant without the ADU (around its equilibrium position of $0.475\ m$) is reduced to $1\ \mu m$. This is the case for the plant including the ADU, after only $1.49\ s$.

B. Closed-loop response

The next step is to look at the influence of the ADU on the closed-loop system. The pole-zero plot of the closed-loop system shows that in the absence of the ADU, the system is unstable for $\omega_c > 12$ rad/s. However, by implementing the ADU, the maximum achievable ω_c increases. Figure 9 shows the performance of the closed-loop system, both with the ADU ($\omega_c = 30\ rad/s$) and without the ADU ($\omega_c = 12\ rad/s$). As expected, the performance of the closed-loop system that includes the ADU is significantly higher than the one without the ADU. Both the overshoot and settling-time are considerably lower, as result of the higher bandwidth.

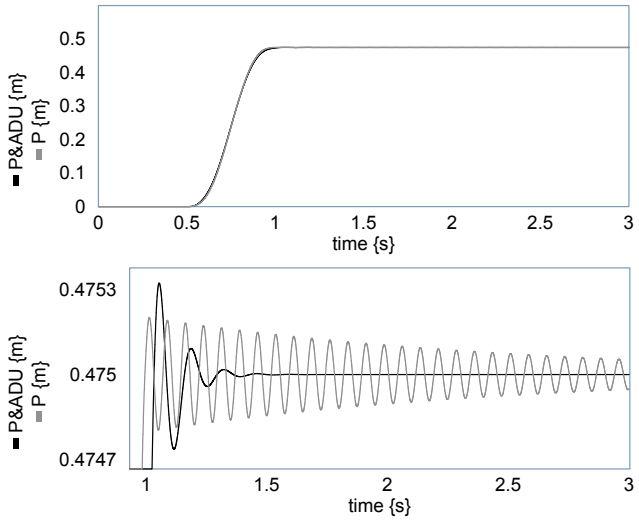

Fig. 8. Simulation of the end-effector position x in time; with acceleration feed-forward force input (no feedback control). Black: no ADU; Gray: with ADU. Top: normal scale, bottom: zoomed in.

The simulation shows that the closed-loop system without the ADU -but with the same bandwidth as the actively damped system ($\omega_c = 30\ rad/s$)- is unstable.

What is clearly observable from the simulations is the significant decrease of the settling time due to the ADU. Table III gives an indication of the system performance for various combinations. In this table, e is the error between the position of the end-effector and the desired position, e_{max} represents the maximum error, t the time in seconds and PID+ the implemented motion controller. The maximum error, e_{max}, is shown for both $0.5\ s$ and $1\ s$ after completion of the motion profile.

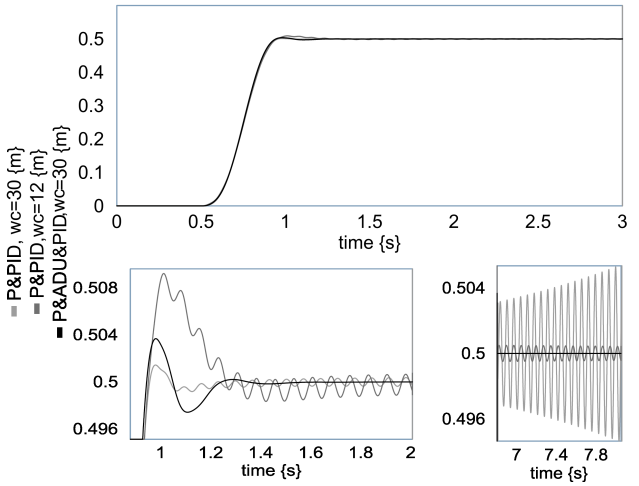

Fig. 9. Simulation of the closed-loop response; x versus time. Black: with ADU, $\omega_c = 30\ rad/s$; Dark gray: no ADU, $\omega_c = 12\ rad/s$; Light gray: no ADU, $\omega_c = 30\ rad/s$. Top: normal scale, bottom: zoomed in.

	e_{max} in mm, after		settling-time s
	$t > 1.5$	$t > 2$	$e < 0.2\ mm$
P & PID+, $\omega_c = 10$	1.53	1.10	14.57
P & ADU & PID+, $\omega_c = 30$	0.10	0.008	1.29

TABLE III
PERFORMANCE OVERVIEW

VIII. CONCLUSIONS

By adding active damping to a plant that suffers from the rocking mode, the maximum achievable bandwidth is increased. This results in a higher performance reflected in lower response and settling times and also in a decrease in the steady-state and/or set-point error. The proposed Active Damping Unit (ADU) guarantees the stability of the actively damped plant by using collocated actuators and sensors in combination with a passive control algorithm. Furthermore, the influence of the model uncertainties have been excluded by only using information about the vibration mode that is to be damped.

REFERENCES

[1] L. Meirovitch, *Principles and techniques of vibration*, Prentice-Hall, Inc., New Jersey, United State of Amerika, 1997.

[2] D.K. Miu, *Mechatronics, electromechanics and contromechanics, an introduction*, Springer-Verlag, Berlin, Germany, 1992

[3] A. Preumont, *Vibration control of active structures*, Kluwer academic publishers, Dordrecht, The Netherlands, 1997.

[4] H.J. Coelingh, *Design support for motion control systems*, Ph.D. thesis, University of Twente, Enschede, The Netherlands, 2000.

[5] J. Holterman, *Vibration control of high-precision machines with active structural elements*, Ph.D. thesis, University of Twente, Enschede, The Netherlands, 2002.

[6] J. van Dijk, J.B. Jonker and R.G.K.M. Aarts, "Frequency domain approach for mechatronic design of motion systems", *submitted to IFAC Mechatronics 2010*.

[7] B. Babakhani and T.J.A. de Vries, "On the stability of P(I)D-controlled motion systems", 5^{th} *IFAC Symposium on Mechatronic Systems*, Cambridge, Massachusetts, United States of America, 2010.

[8] D. Borger, *On the stability properties of motion controllers*, M.Sc. report, University of Twente, Enschede, The Netherlands, 2002.